Electron spin resonance and nuclear magnetic resonance

2197055

Abstract. Electron spin resonance (ESR) and nuclear magnetic resonance (NMR) are two important spectroscopic techniques for probing properties of materials containing constituents with non-zero permanent magnetic moments capable of resonant absorption of electromagnetic energy — electronic systems in the case of ESR and atomic nuclei in the case of NMR. In this experiment, we studied ESR on a sample of Diphenyl-Picryl-Hydrazil (DPPH), a paramagnetic organic molecule with an unpaired e^-, by means of measuring the resonant frequency as a function of externally applied magnetic field in order to determine the sample's g-factor, which was found to be $g_{\mathrm{DPPH}} = 2.02 \pm 0.01$. Further, we investigated the magnetic properties of ^{1}H and ^{19}F nuclei in the following substances: glycerine, polystyrene (both of which contain hydrogen), PTFE (which contains fluorine), and polythene, whose composition we wanted to infer. The experimentally measured g-factors were $g_{\mathrm{glycerine}} = 5.54 \pm 0.03$, $g_{\mathrm{polystyrene}} = 5.68 \pm 0.01$ and $g_{\mathrm{PTFE}} = 5.34 \pm 0.01$. Comparison with the results obtained for polythene lead us to postulate the presence of hydrogen in our polythene sample, as confirmed by its chemical formula.

1. Introduction

Electron spin resonance (ESR), also referred to as electron paramagnetic resonance (EPR) spectroscopy, is an important method for studying paramagnetic chemical substances, in which the electrons' magnetic moments don't cancel, such as organic and inorganic free radicals or transition-metal ion complexes. It can provide detailed information relating to the chemical composition and structure of materials, and therefore finds innumerable applications in biology, chemistry, materials science, medicine and pharmacology, to name just a few.

Similarly, nuclear magnetic resonance (NMR) exploits the fact that some nuclei possess a non-zero overall spin, and hence a permanent magnetic moment, to probe the properties of materials containing such nuclei. It has widespread use and far-reaching applications, notably in medical imaging, where it forms the basis behind MRI (magnetic resonance imaging).

The aim of this experiment was to explore the fundamental principles underlying these two phenomena.

2. ESR

In the first part of the experiment, we performed an ESR study on a sample of Diphenyl-Picryl-Hydrazil (DPPH), which is a paramagnetic organic molecule with a single unpaired e^-. The orbital angular momentum of this electron is essentially zero, and hence the molecule's total magnetic moment is solely due to the electron's intrinsic spin angular momentum, which makes it particularly suited for ESR investigations.

2.1. Theory

In the absence of any external magnetic fields (i.e. for a free e^-), the two possible spin states ("spin up" and "spin down") are degenerate — they have the same energy.

However, energy *splitting* of the two states occurs when the electron is placed in a magnetic field. Indeed, the electron's spin gives rise to a magnetic moment $\boldsymbol{\mu}_S$ which interacts with the applied field and possesses a different energy depending on its relative spatial orientation.

According to quantum mechanics, only two configurations are possible. The magnitude S of the spin vector, $\mathbf{S}$, and its two allowed z-components S_z (where the z-axis is defined to lie along the direction in which the field is pointing), are respectively given by

$$S = ||\mathbf{S}|| = \sqrt{s(s+1)}\hbar = \frac{\sqrt{3}}{2}\hbar, \quad \text{and}$$
$$S_z = m_s\hbar. \tag{2.1}$$

where $s = \frac{1}{2}$ is the spin quantum number, $m_s = \pm\frac{1}{2}$ is the secondary spin quantum number, and $\hbar = \frac{h}{2\pi}$ is the reduced Planck's constant.

The associated magnetic moment is

$$\boldsymbol{\mu}_S = -g\frac{\mu_B}{\hbar}\mathbf{S} \tag{2.2}$$

where g is the Landé splitting factor, or g-factor, which for a free electron has the value $g_e = 2.002319$, and $\mu_B = 9.274 \times 10^{-24}\,\mathrm{J\,T^{-1}}$ is the Bohr magneton. Note that the magnetic moment points in the opposite direction as the spin vector $\mathbf{S}$ due to the electron's negative charge.

A magnetic moment in a field $\mathbf{B} = B\,\mathbf{e_z}$ (where $\mathbf{e_z}$ is the unit vector in the z-direction) has potential energy

$$E = -\boldsymbol{\mu}_S \cdot \mathbf{B} = -(-g\frac{\mu_B}{\hbar}\mathbf{S}) \cdot \mathbf{B}, \quad \text{substituting in from (2.2),}$$
$$= g\frac{\mu_B}{\hbar}S_z B, \quad \text{using (2.1),}$$
$$= g\mu_B m_s B. \tag{2.3}$$

Equation (2.3) shows that the two orientations ($m_s = \pm\frac{1}{2}$) no longer have the same energy — the one whose magnetic moment is aligned with the field (or equivalently whose spin points in the direction opposite to the field, i.e. having $m_s = -\frac{1}{2}$) has a lower potential energy than the one whose magnetic moment is anti-parallel to the field —, as depicted in figure 2.1. The energy difference between the two levels is

$$\Delta E = g\mu_B B. \tag{2.4}$$

In thermal equilibrium, the spins are distributed according to the Boltzmann distribution

$$\frac{N_{+\frac{1}{2}}}{N_{-\frac{1}{2}}} = \exp(-\frac{\Delta E}{k_B T}),$$

where k_B is Boltzmann's constant, and $N_{\pm\frac{1}{2}}$ are the number of spins in the higher and lower states, respectively.

If there are more spins in the lower than the upper state, transitions can be induced by supplying energy, e.g. by irradiating the sample with electromagnetic (EM) radiation with the
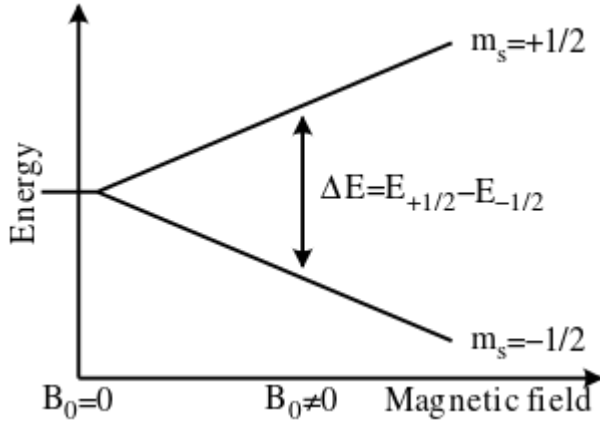
Figure 1. Energy splitting of the two spin states of an e^- placed in an external magnetic field $\mathbf{B_0}$.

right frequency ν. The energy of an EM wave is $E = h\nu$, where h is Planck's constant, so the condition for resonance, given (2.4), can be stated as

$$h\nu = g\mu_B B. \tag{2.5}$$

In a real material, an electron "feels" not only the externally applied field, but also the fields produced by any surrounding (magnetic) nuclei and/or other electrons. The effect of the surroundings can be interpreted as a shift in the g-value that appears in equation (2.2) compared to the free-electron value. In addition, the chemical environment also has an effect on the shape of the resonance signal and its line width, amongst other things. This gives an indication of how ESR can be used to infer information on the chemical composition and structure of materials. In this particular experiment, we measured the g-value of DPPH.

2.2. Experimental method
The DPPH sample was placed in a uniform magnetic field generated by two parallel vertically-positioned Helmholtz coils (HCs) connected to a DC current supply. The sample was inserted into another coil connected to an RF circuit oscillating at an adjustable frequency ν. This coil provided the energy $h\nu$ needed to flip the e^-s spins. The magnetic field produced by the HCs was varied, by changing the current, to identify when the resonance condition (2.5) was met for a particular (fixed) frequency. The measurement was then repeated for a number of different frequencies. The resonance was detected thanks to a measurable voltage change in the RF circuit, observed using an oscilloscope, that occurred due to the change of the RF coil's permeability when the sample was absorbing energy. (The magnetic field induced in the RF coil was perpendicular to the field of the HCs and was neglected for the purposes of the results analysis).

For an e^- with only two possible spin states, it would be necessary to match the RF frequency and the current in the HCs with considerable accuracy to obtain resonance. Also, once the population of the spin states has been inverted, the sample can no longer absorb more energy before enough electrons have returned to the lower state, so they need to be excited at a rate slower than the relaxation time (the time needed for the electrons to de-excite and return to thermal equilibrium via spin-spin and spin-lattice interactions). The solution to both problems was to superimpose a (50Hz) modulation (AC) current on the DC component going into the HCs, resulting in a sinusoidally-varying modulation magnetic field. The total field $\mathbf{B}_{total}$ was then the superposition of the two, and thus oscillated around a central value B_0. If the resonance condition (2.5) was satisfied for some value of $\mathbf{B}_{total}$ during this oscillation, a resonance signal was observed, twice during the cycle at symmetric positions (provided that the phase lag between

the modulation signal and the sample response signal was correctly accounted for). By adjusting the DC current, it was possibly to make the resonance occur precisely at the point when the modulation field dropped to zero and the field was equal simply to B_0, i.e. it was the B_0 that satisfying (2.5) for the given frequency.

The value of B_0 could be deduced from the DC current I_0 in the coils — we created a calibration curve of B_0 as a function of I_0 using a Hall probe sensor to measure the magnetic field in the centre of the coil set-up.

2.3. Results
The results of the two stages of the experiment are summarized in the following subsections.

2.3.1. Helmholtz coils calibration.
The direct current going through the Hemlhotz coils was varied and the magnetic field B_0 at the centre of the coils was recorded. We observed quite large fluctuations of the field for a given current, and therefore 5 different readings were taken and averaged. For the purposes of error analysis, the uncertainty in the mean was then taken to be half the spread of the observed values (as there weren't enough readings to justify using the formula for the standard error in the mean). For the current, the measurement uncertainty was taken to be half the smallest scale division.

We subsequently performed a weighted straight-line fit to the data. Figure 2.3.1 shows the resulting calibration curve with uncertainties indicated by error bars. This curve was used in the second part to convert between measured current and magnetic field applied to the sample. We used the MATLAB's built-in function `polyval` to estimate the uncertainties in the values of B_0 predicted by the curve, based on the goodness of fit.

We obtained
$$B_0 = (3.73 \pm 0.01)I + (0.03 \pm 0.01),$$
where I is in A, and B_0 is in mT.

2.3.2. Measurement of the g-factor of DPPH.
The frequency in the RF oscillator circuit was varied in steps of 5MHz, and for each frequency, the current in the Helmholtz coils was scanned over the range 0.1A to 1.2A to find the resonance. For a given frequency, the measurement was repeated multiple times to get an idea of the uncertainty in the resonant current. Figure 2.3.2 shows the resonance frequency as a function of the field.

2.4. Analysis
According to equation (2.5), the plot of frequency ν against magnetic field B_0 should be a straight line with gradient
$$\frac{\nu}{B_0} = \frac{g_{\text{DPPH}}\mu_B}{h},$$
which implies
$$g_{\text{DPPH}} = \left(\frac{h}{\mu_B}\right)\left(\frac{\nu}{B_0}\right). \tag{2.6}$$

From the weighted straight-line fit to our data shown in figure 2.3.2, we have
$$\left(\frac{\nu}{B_0}\right) = 28.24 \pm 0.07 \text{ MHz mT}^{-1}.$$

Substituting into (2.6) yields

$$g_{\mathrm{DPPH}} = 2.02 \pm 0.01,$$

(where the uncertainty in the final value has been computed, given that h and μ_B are constants, simply by multiplying the error in the gradient by h/μ_B).

2.5. Discussion

For a pair of Helmholtz coils separated by a distance equal to their radius, electromagnetic theory predicts that the value of the field at the centre should obey approximately

$$B_0 = \mu_0 \left(\frac{4}{5} \right)^{\frac{3}{2}} \frac{n}{r} I,$$

where $\mu = 4\pi \times 10^{-7} \,\mathrm{V\,s\,A^{-1}\,m^{-1}}$, n is the number of turns per coil, and r is their radius.

This shows that the expected relationship between I and B_0 was linear, as confirmed by our data (see figure 2.3.1). However, for our particular coils, the expected value of the gradient was 4.23, which does not agree with the value that we obtained experimentally, i.e. 3.73 ± 0.01. This could be due to the fact that the separation of the coils might not have been exactly equal to their radius. Due to such possible differences in our set-up from the idealised case, we used the experimentally obtained calibration curve in the subsequent sections, not the theoretical one. Any error in the calibration curve therefore represents a systematic error in the results obtained thereafter.

Possible sources of error were the difficulty in making sure that the Hall probe was oriented perpendicularly to the measured field (i.e. parallel to the coils), and that it was located at the exact position where the sample was later placed. We also couldn't be sure whether the Hall probe itself was calibrated correctly (as we didn't obtain the expected result when we checked with a standard magnet), and whether we zeroed it at a point with no magnetic field. This could have introduced a systematic offset. A source statistical errors were the random fluctuations in the magnetic field and in the response of the probe over time (e.g. due to warming up of the equipment).

Our measurement of the DPPH resonance confirmed the linear relationship predicted by (2.5) for the magnetic field and the resonance frequency. This shows that, indeed, an energy splitting occurs when the sample is placed in an external field, that this creates two separate energy levels such that the energy difference between them scales linearly with the applied field, and that energy transitions can be induced by supplying EM energy of the correct frequency.

The accepted value for the g-factor of DPPH is

$$g_{\mathrm{DPPH,\ th}} = 2.0036.$$

Our value lies within 2σ of this value, and is therefore in reasonable agreement. Compare this with the theoretical value for the g-factor due to the spin of a free e^-

$$g_{e,\ \mathrm{th}} = 2.002319.$$

This is slightly different from both the accepted and our experimental value for g_{DPPH}, which, as explained in the (2.1) theory section, could stem from the effect of the chemical surrounding of the unpaired e^-. Nevertheless, the values are relatively close, showing in particular that the assumption that we can neglect the orbital angular momentum of the e^- and attribute the molecule's magnetic moment solely to the spin angular momentum was largely justified.

An increase in the precision of our measurements could have been achieved by taking further repeated measurements for a given set of conditions in order to deal with statistical errors due to

random fluctuations, but also by using a stronger **B** field, thus increasing the energy difference between the two spin states and hence reducing the relative uncertainty in this difference, and/or by operating at lower temperatures, both of which would possibly result in a sharper resonance signal (i.e. a reduced line width).

3. NMR

In the second part of the experiment, we performed NMR on protons and fluorine atoms in both liquid and solid samples, namely in glycerine and polystyrene (which contain ^{1}H), PTFE (containing ^{19}F), and polythene, about which we wanted to determine whether it is more likely to contain hydrogen or fluorine.

3.1. Theory

The basic principles of NMR are essentially the same as those of ESR. Atomic nuclei that have an odd number of nucleons can have a non-zero overall nuclear spin **S** which gives rise to a nuclear magnetic moment $\boldsymbol{\mu}_n$. When placed in a magnetic field, either external, or due to other close-by magnetic nuclei or the orbiting electrons, the nuclear spin can adopt, quantum-mechanically speaking, $2S + 1$ possible orientations, each corresponding to a different energy level

$$E_n = -g\mu_n B_0 n, \quad n = -S, -S + 1, \ldots, 0, \ldots, S.$$

The g-factor again depends on the chemical environment and bond structure (so-called "chemical shift").

All of our samples had $S = \frac{1}{2}$, which meant there were only two possible spin levels, and the condition for resonance was

$$h\nu = \Delta E = -g\mu_n B0. \tag{3.1}$$

3.2. Experimental method

The experimental procedure was analogous to the ESR part of the experiment (see section (2.2)). The only differences were that the static magnetic field was generated by an iron-cored electromagnet, instead of Helmholtz coils, and the modulating field was produced by a pair of smaller attached modulation coils.

3.3. Results

3.3.1. Electromagnet calibration. Just like in section (2.3.1), we first calibrated our electromagnet to be able to relate current passing through it to the magnetic field. Since the electromagnet contained an iron core, its field depended not only the value of the current, but also on whether the current was being increased or decreased. This effect is called *hysteresis* (a dependence of the net magnetization of a ferromagnet on the history of any externally applied magnetic field).

Therefore, we did our calibration first for an increasing and then a decreasing current. Figure **??** shows the hysteresis curve obtained.

Note. *Only the part of the curve corresponding to increasing current was used in the next section.*

We fitted a polynomial of degree 2, $y = ax^2 + bx + c$, to the upper half of the curve (this was the degree that yielded the lowest error estimates on the fit parameters), with

$$a \approx -16 \pm 1,$$
$$b \approx 189 \pm 7,$$
$$c \approx -34 \pm 12.$$

3.3.2. Measurement of the g-factors of Glycerine, Polystyrene and PTFE. Figure **??** shows the graphs of resonance frequencies as a function of B_0 for the 3 different substances, and figure **??** shows the general shape of the resonance signals as viewed on an oscilloscope.

3.4. Analysis

According to (3.1), $\left|\frac{\nu}{B_0}\right|$ should be a constant, equal to $\frac{g\mu_n}{h}$. It follows that $g = \frac{h}{\mu_n}\left(\frac{\nu}{B_0}\right)$. We performed a straight-line fit to our plots in figure **??**, and got

$$\left(\frac{\nu}{B_0}\right)_{\text{glycerine}} = 0.0422 \pm 0.0002 \ \text{MHz}\,\text{mT}^{-1}$$

$$g_{\text{glycerine}} = 5.54 \pm 0.03$$

$$\left(\frac{\nu}{B_0}\right)_{\text{polystyrene}} = 0.0433 \pm 0.0001 \ \text{MHz}\,\text{mT}^{-1}$$

$$g_{\text{polystyrene}} = 5.68 \pm 0.01$$

$$\left(\frac{\nu}{B_0}\right)_{\text{PTFE}} = 0.0407 \pm 0.0001 \ \text{MHz}\,\text{mT}^{-1}$$

$$g_{\text{PTFE}} = 5.34 \pm 0.01$$

3.5. Discussion

4. Conclusion

References

[1]